

## Dynamic Behavior of Moving Coil Type Control Rod Drive Mechanism

Osamu KOJIMA

*NKK Corporation, Kawasaki, Japan*

Mitsuo TAKEUCHI, Masaji TAKAYANAGI

*Japan Atomic Energy Research Institute, Tokaimura, Japan*

Takashi KANAZAWA

*NKK Corporation, Yokohama, Japan*

Kengo TAGAWA

*Fukui University, Fukui, Japan*

### ABSTRACT

This paper deals with the vibration tests and seismic response analyses on a newly devised moving coil type CRDM which is installed in the Upgraded JRR-3. The dynamic properties of the CRDM and the relationship between the scram time and the maximum deflection of the lower guide pipe are obtained. Then, it is confirmed that the structural strength and function of the CRDM during earthquakes is satisfactory.

### 1 INTRODUCTION

The Japan Research Reactor No.3 (JRR-3), which was constructed by the Japan Atomic Energy Institute in 1962, has been upgraded and completed in 1990 as shown in Fig. 1. A new type of Control Rod Drive Mechanism (CRDM) is installed in the Upgraded JRR-3. The CRDM is a means to change the position of each control rod, which consists of neutron-absorbing medium, relative to the reactor core so as to control the reactor output. Therefore, it plays the most important role in ensuring the safety of the reactor.

In seismic design codes such as Technical Guidelines for Aseismic Design of Nuclear Power Plants, stringent guidelines for the CRDM are divided into two primary areas: to be free of primary coolant leakage, and to have high scram function reliability.

### 2 CONTROL ROD DRIVE MECHANISM

In this type of CRDM, the strong electromagnetic body (plunger) attached to the control rod is driven magnetically, corresponding to the movement of the electromagnetic coil (magnet) located around the exterior of the lower guide pipe as schematically drawn in Fig. 2. Because there is no sealing section in the lower guide pipe, which penetrates the reactor coolant boundary, coolant leakage is eliminated. The scram function can be attained through demagnetization, resulting in the free-fall of the plunger.

### 3 VIBRATION TESTS

#### 3.1 Test method

Forced vibration tests and scram function tests were performed by using a shaking SMiRT 11 Transactions Vol. C (August 1991) Tokyo, Japan, © 1991

table. Among the 6 units of CRDM, one unit was installed in the test setup, which simulated the Upgraded JRR-3, as shown in Fig. 3. The remaining 5 units were modeled as added mass. Acceleration pickups, a displacement transducer and strain gauges were attached as indicated by the symbols of  $\circ$ ,  $\rightarrow$  and  $\parallel$  respectively to measure the dynamic properties of the CRDM. The position of the CRDM was changed as a main test parameter; lower, 250mm, middle, and upper. The seismic lateral deflection of the CRDM stay is assumed to be at maximum in the lower position. Meanwhile, that of the lower guide pipe is assumed to be at maximum in the 250mm or middle position. Additionally, that of the upper guide pipe is assumed to be at maximum in the upper position.

In the forced vibration tests, sinusoidal waves with a frequency range from 5 to 20 Hz and round time of 14 minutes were excited. In the scram function tests, sinusoidal waves and random waves were excited. The sinusoidal waves have 5 levels of magnitude with the same components as the natural frequency of the lower guide pipe. The random waves are the floor response accelerations of the Upgraded JRR-3, which will be caused by S1 (the maximum possible earthquake) and S2 (the maximum probable earthquake). The CRDM was shaken in two directions as shown in Fig. 3(b).

### 3.2 Results of forced vibration tests

Natural frequencies and critical damping ratios of the guide pipe and the CRDM stay in the shaking direction 1 were derived from the measured resonance curves, and they are tabulated in Table 1. The natural frequencies of the guide pipe are different according to the position of the CRDM. Meanwhile, that of the CRDM stay is almost the same at any CRDM position. Additionally, it is found that the effect of orthogonal shaking upon the dynamic properties of the CRDM is negligibly small.

The natural frequency of the guide pipe at any position of the CRDM is more than two times higher than that of the Upgraded JRR-3 (4.3Hz). The critical damping ratio of the guide pipe is greater than the value adopted in the conventional seismic design of general piping equipment. For these reasons, the magnification factor of the CRDM appeared to be small in the seismic response.

Natural vibration modes of the guide pipe and the CRDM stay in the case of the middle position of the CRDM and the shaking direction 1 are depicted by the symbols of  $\circ$  and  $\triangle$  in Fig. 4. The coupling modes of the lower guide pipe and the CRDM stay are observed.

### 3.3 Results of scram function tests

Measured data during the free-fall of the control rod is displayed in Fig. 5, which were recorded from the upper position of the CRDM and the shaking direction 1 under the S2 excitation.

The relationship between the scram time and the maximum deflection of the lower guide pipe is obtained in Fig. 6. The scram time is defined as a time from scram start until the time of 80%-drop of drop stroke. The scram time under the random waves is found to be within the acceptable level of one second, and it is almost the same as under the sinusoidal waves. Additionally, the scram time under the excitation stronger than the S2 is almost the same as that under static conditions.

Through a total of 432 scram function tests, it is verified that the scram function of this type of CRDM during earthquakes is highly reliable.

## 4 RESPONSE ANALYSES

### 4.1 Modeling

The properties of the guide pipe and the CRDM stay are tabulated in Table 2. For the seismic response analysis, they are modeled as a lumped-mass system, including

flexural-shear beam elements and spring elements as shown in Fig. 7. The coupling of the lower guide pipe and the CRDM stay through the magnet is represented by equivalent spring elements with spring constant  $K_1$  and  $K_2$ . The spring constant  $K_3$  represents the rigidity of the gasket, and  $K_4$  does that of the aseismic support frame. The mass of the magnet is distributed about 40% in the lower guide pipe, and about 60% in the CRDM stay. Inner pipe components are treated only as nodal masses.

In the modeling of the upper guide pipe, the gap from the support sheath is substituted by equivalent spring elements with spring constant  $K_1$  and  $K_2$ . Here, inner pipe components are also treated only as nodal masses.

#### 4.2 Eigen-value analysis and response analysis

In order to investigate the validity of the modeling of the CRDM, the results of Eigen-value analysis are compared with those of the tests. The analytical Eigen-values are put down in the parenthesis in Table 1. The analytical mode shapes are drawn in solid lines in Fig. 4. Fairly good agreements are obtained between the test and analysis, and the modeling is confirmed to be appropriate.

The computed responses of shear forces and bending moments were compared with those measured during the scram function tests in the case of the middle position of the CRDM and the shaking direction 1 under the S2 excitation, as shown in Fig. 8. Fairly good agreements are also observed.

The sum of the seismic stress and the primary stress, mainly caused by inner pressure, is within the allowable stress. Therefore, the structural strength of the CRDM under the S1 and S2 excitation is ascertained to be satisfactory.

### 5 CONCLUSIONS

The following conclusions were drawn from the results of this study:

- 1) Dynamic properties of the CRDM are obtained; the natural frequency of the guide pipe at any position of the CRDM is more than two times higher than that of the Upgraded JRR-3 (4.3Hz). Accordingly, this type of CRDM is verified to be a rigid structure.
- 2) The relationship between the scram time and the maximum deflection of the lower guide pipe is obtained. Accordingly, the scram time under the random waves is verified to be within the acceptable level of one second. The scram time under the excitation stronger than the S2 is almost the same as that under static conditions.
- 3) From the comparison between the Eigen-value analysis and test results, an appropriate coupling model of the lower guide pipe and the CRDM stay is constructed. By using this model, fairly good agreements are observed between the test results and the seismic response analyses.
- 4) It is confirmed that the structural strength and function of the CRDM under the S1 and S2 excitation is satisfactory.

### ACKNOWLEDGEMENTS

The authors are especially grateful to Prof. H. Shibata of Tokyo University, who has provided persevering guidance during the vibration tests of the CRDM.

### REFERENCES

- Shibata, T. et al. (1982). Moving Coil Type Control Rod Drive Mechanism. Nippon Kokan Technical Report, Overseas No.35, pp. 83-92.
- Takeuchi, M. et al. (1987). Vibration Examination of CRDM for Upgraded JRR-3. Fall Meeting of the Atomic Energy Society of Japan, p.182.

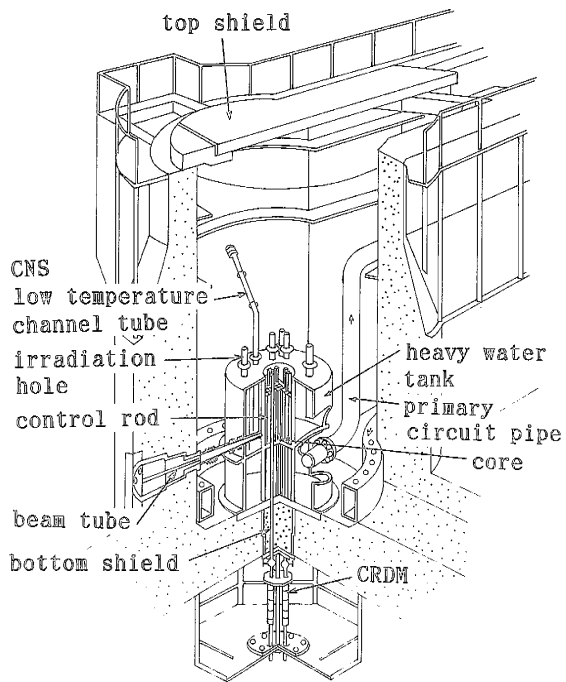


Fig. 1. Isometric view of the Upgraded JRR-3

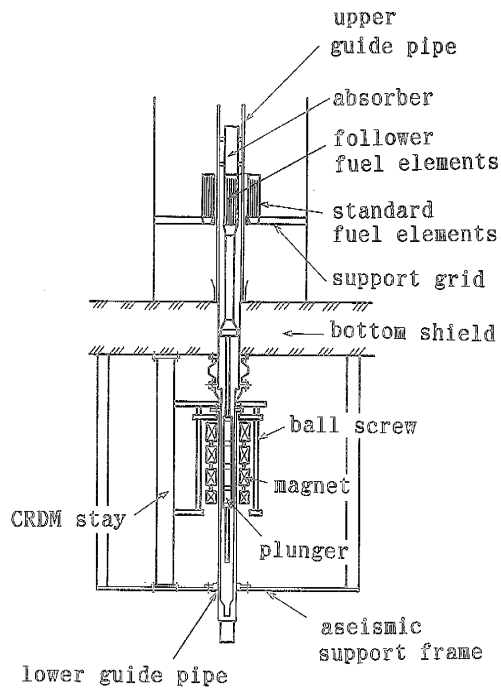
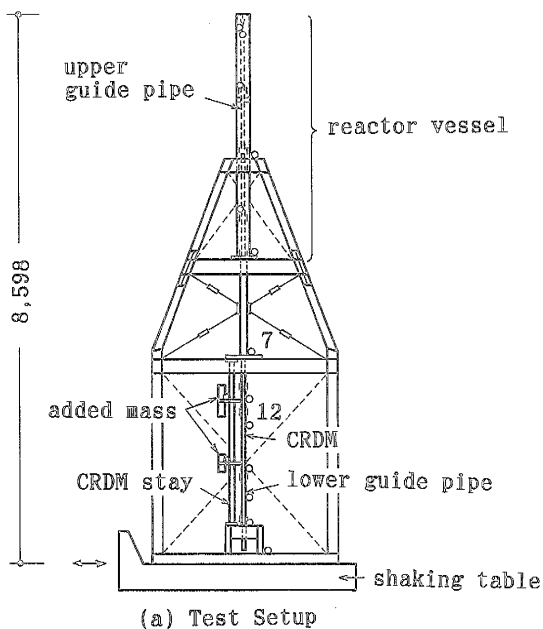
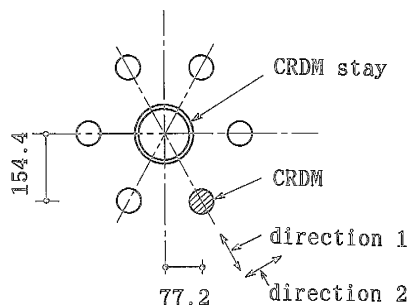


Fig. 2. Schematic drawing of the CRDM



(a) Test Setup

- acceleration pickup
- displacement transducer
- strain gauge



(b) Shaking Direction

Fig. 3. Test method

Table 1. Dynamic properties of the CRDM (shaking direction : 1)

Position of CRDM	Lower guide pipe		CRDM stay		Upper guide pipe	
	Natural frequency (Hz)	Damping ratio (%)	Natural frequency (Hz)	Damping ratio (%)	Natural frequency (Hz)	Damping ratio (%)
Lower	16.7~17.0(17.0)*	3.4	18.0~18.5(18.9)	1.9	18.4 (18.5)	2.2
250 mm	12.5~13.0(13.4)	4.8	17.5~18.0(18.4)	1.5	18.3 (18.5)	1.9
Middle	12.5~13.0(13.5)	5.0	17.6 (18.4)	1.7	18.1 (18.3)	2.6
Upper	16.5~17.0(16.3)	—	17.5~18.0(19.0)	—	16.5~17.0(14.2)	4.0

\*analytical values are in parenthesis

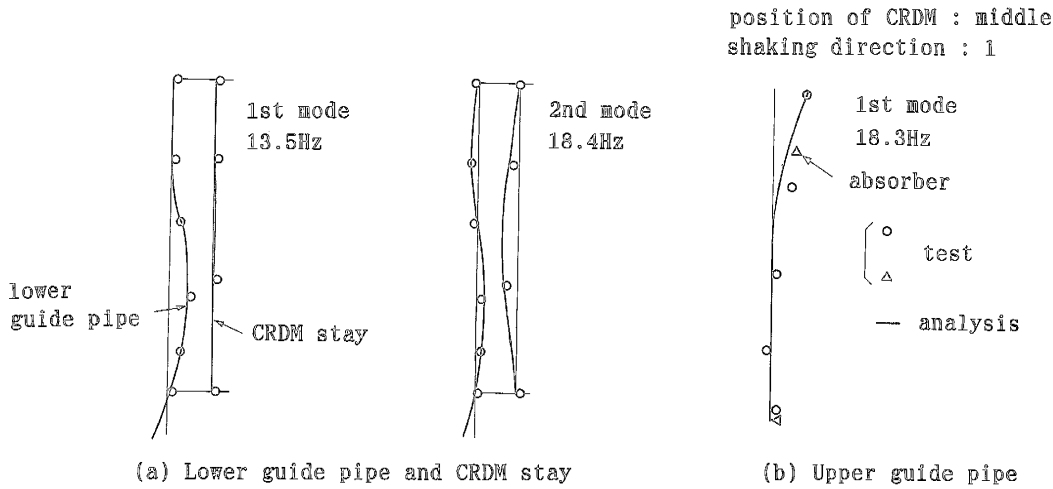


Fig. 4. Mode shapes of the CRDM

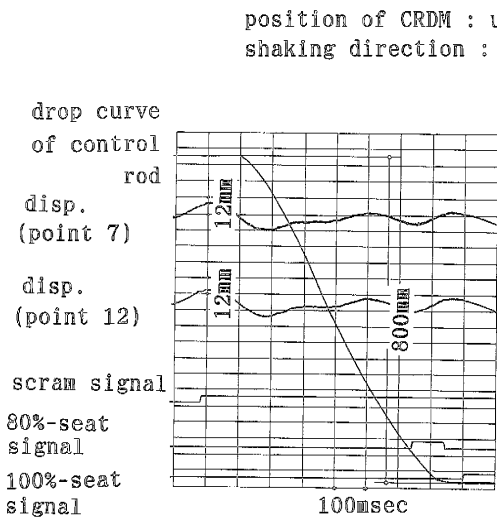


Fig. 5. Measured data during scram function test

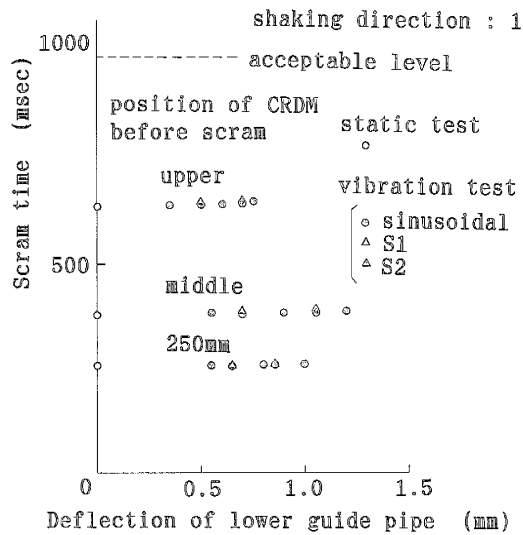


Fig. 6. Scram time vs. deflection of lower guide pipe

Table 2. Properties of the CRDM

	Lower guide pipe CRDM stay		Upper guide pipe
Material	SUS304L	SUS304	A6063S-T5
Dimension(mm)	$\phi 48.6 \times t 2.3$	$\phi 89.1 \times t 7.6 \sim \phi 101.6 \times t 8.1$	$\square 76.2 \times t 5.0$
Weight(kg/mm)	$4.61 \times 10^{-3}$	$1.54 \times 10^{-2} \sim 1.89 \times 10^{-2}$	$3.85 \times 10^{-3}$
Sectional area(mm <sup>2</sup> )	$3.35 \times 10^2$	$1.95 \times 10^3 \sim 2.38 \times 10^3$	$1.42 \times 10^3$
Moment of inertia(mm <sup>4</sup> )	$8.99 \times 10^4$	$1.63 \times 10^6 \sim 2.62 \times 10^6$	$1.21 \times 10^6$
Young's modulus (kg/mm <sup>2</sup> )	(20°C) 19,900 (75°C) 19,600	(20°C) 19,900 (50°C) 19,700	(20°C) 7,000 (100°C) 6,900
Poisson's ratio	0.3	0.3	0.33

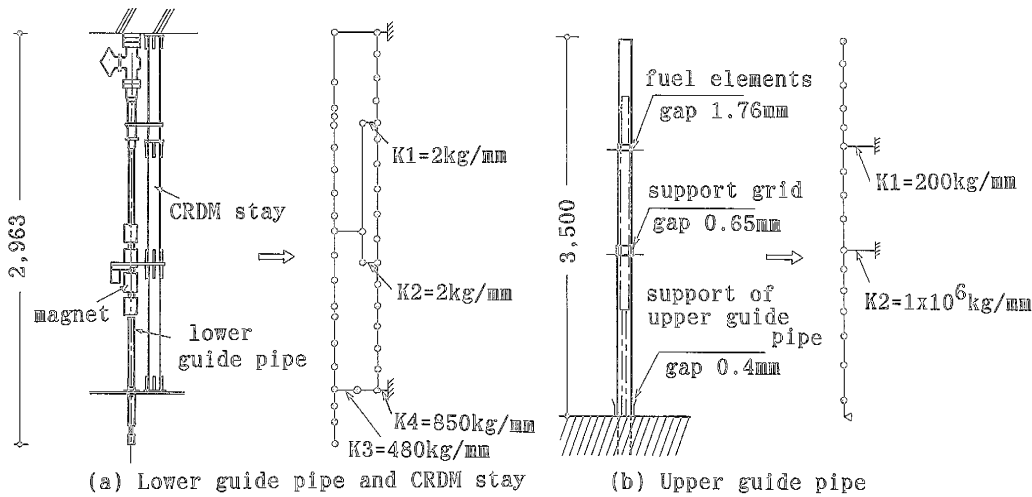


Fig. 7. Modeling of the CRDM

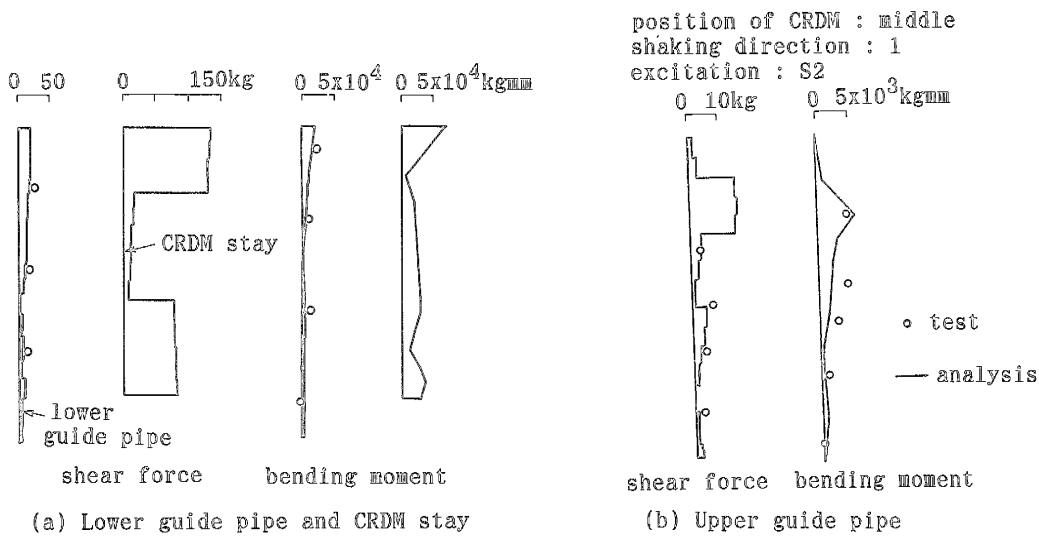


Fig. 8. Seismic responses of the CRDM